Journal of Applied Fluid Mechanics, Vol. 12, No. 3, pp. 743-749, 2019.
Available online at www.jafmonline.net, ISSN 1735-3572, EISSN 1735-3645.
DOI: 10.29252/jafm.12.03.29170

An Investigation on the Effect of Blade Tip Clearance on the Performance of a Single-Stage Axial Compressor

M. Ostad and R. Kamali†

Department of Mechanical Engineering, Shiraz University, Shiraz, I. R. of Iran

†*Corresponding Author Email: rkamali@shirazu.ac.ir*

(Received May 5, 2018; accepted October 29, 2018)

ABSTRACT

In the present study, the numerical analysis of blade tip geometry effect on the performance of a single-stage axial compressor has been the focus of attention. The studied geometries included a rotor with variable tip clearance. For the first model, the tip clearance increases as it moves toward the blade trailing edge. The tip clearance of the second model reduces as it approaches the trailing edge, whereas in the third model, the tip clearance remains constant. The results indicated that the tip clearance of the first sample, as the worst tip clearance case, creates a 10% reduction in the stall margin with respect to the third standard model, and the second sample tip clearance brings about a stall margin reduction of 4% efficiency with respect to the third standard model. Then, the effect of blade tip clearance geometry on outlet flow angle of the rotor was inspected. The results showed that in the first model, the outlet flow angle has the largest deviation than the third standard model and the second model performance places somewhere between the two other tip clearance geometries. Also evident from the result is that taking advantage of the variable blade tip clearance is not an appropriate method for improving compressor performance.

Keywords: Axial compressor; Variable tip clearance; Stall margin; Flow angle; Compressor performance.

1. INTRODUCTION

Of various factors influencing the flow in multi-stage compressors, tip clearance always plays the most vital role the integrity of the flow in rotor cascade (Domercq *et al.*, 2007). The results presented by Ivey *et al.* indicated that the increase of blade tip clearance causes highly important changes on stator's downstream and the rise in stator's loss is due to the choking flow increase on the compressor's wall, resulting from the tip clearance expansion (Howard *et al.*, 1994; Foley *et al.*, 1996). Smith and Key, analyzed the observed details in a multi-stage compressor and noticed that the tip clearance size has a serious impact on 3-D passage flow separation of stator in nominal load conditions (the design point flow rate) (Smith *et al.*, 2015).

The existence of tip clearance in a compressor is inevitable and it should actually exist as a definite space between the moving parts and stationary casing wall. Nevertheless, it has been studied from a long time ago due to its immoderate loss on the compressor performance, and in particular, on the compressor performance in stall condition and researchers have tried to minimize the tip clearance loss by understanding the effects of tip clearance on the flow inside a compressor. Numerous methods such as implementing casing treatment (Kim *et al.*, 2013), swept and leaned blades (Kroger *et al.*, 2011), utilizing winglet on the suction side of blade (Han *et al.*, 2011; Zhong *et al.*, 2011) and using vertical impact jet (Bae *et al.*, 2003) have been proposed to control the tip clearance flow and to achieve higher stability and better overall efficiency in the compressor.

(Zhong *et al.*, 2013) experimentally studied the effect of winglet on a cascade and concluded that the location of winglet has a considerable influence on the vortex produced as a result of blade tip leaked flow, and that the placement of winglet on the suction side proves effective in reducing the total outlet pressure and the secondary flow as a result of leakage flow from the tip clearance (Zhong *et al.*, 2013). Using this type of winglet was essentially presented by Whitcomb in 1976 to control vortex on the blade tip. Bianchi *et al.* used the placed profiles on the bottom of blade tip to reduce noise in an axial fan (Corsini *et al.*, 2006; Bianchi *et al.*, 2008; Corsini *et al.*, 2008). Sitaram and Sivakumar (2011) investigated the flow field on the rotor outlet for an axial fan with a low aspect ratio and analyzed the effect of various rotor tip geometries on flow coefficients. They

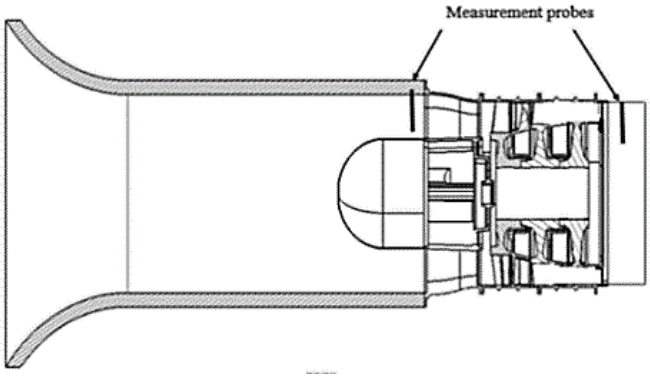

Fig. 1. A view of the cross section of investigated compressor.

observed that the partial shrouds in the blade tip region, plays a significant role on the reduction of low velocity regions near the blade tip (Sitaram *et al.*, 2011).

The purpose of the current study is to evaluate the effects of different rotor blade tip geometries on the performance of compressor stage and to discuss the impact of such geometries on the performance of compressor stage.

2. TEST SECTION

The considered compressor includes one stage of rotor and stator, in addition to one stage of inlet guide vane for which the geometrical properties has been presented in Table 1. As can be seen in Fig. 1, bellmouth geometry was incorporated for uniform flow inlet to the compressor, and the location of pressure and temperature probes to measure the pressure and temperature was decided to be at the beginning and at the end of compressor.

Table 1 Specification of compressor's stage

Blade type	Number
IGV Blade	3
First rotor blades	23
First stator blades	49

The measured data at the inlet and outlet of the compressor includes stagnation pressure and temperature in those areas. Such data were measured at a rotational velocity of 28015 revolutions per minute.

3. MESH GENERATION

To extract the exact numerical results, the structured mesh sample in the computational domain was used and the best grid regarding the turbulence model was applied on the geometry. After creating a suitable 3-D geometry, the software TURBOGRID was used to create a computational grid which took advantage of j/l/c grid topology and boundary layer settings. Because of observing the effects of boundary layer, the mesh around the blade became so small and using the settings of mentioned software, a value of $y^+<5$ was considered.

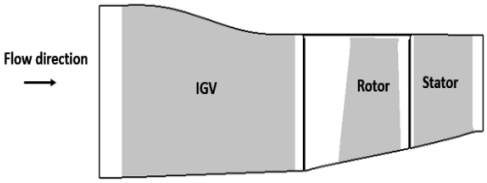

Fig. 2. Meridional view of compressor's stage.

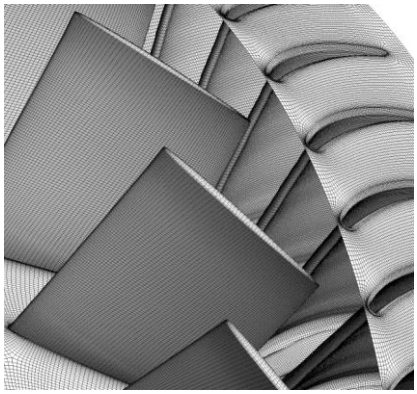

Fig. 3. A view of the generated mesh.

4. GOVERNING EQUATIONS

One of the major problems in turbulence modeling, is accurately predicting the flow separation from smooth plates. The standard two-equation turbulence models usually present a wrong prediction of starting point and the value of flow separation in adverse pressure gradient conditions. This is a serious phenomenon in numerous technical applications, especially in aerodynamic problems in which the stall characteristics are controlled by flow separation. Consequently, turbulence models have become more sophisticated for such applications. In general, the turbulence models based on ε equations, predict the start of flow separation much later and offer a weak prediction for the upcoming flow separation. To numerically analyze the effects of tip clearance on the blade performance, the k-ω turbulence model was used so that a better prediction is achieved regarding

the flow separation location and compressor performance, although there are cases for which one-equation Spalart Allmaras turbulence model was employed (Kim *et al.*, 2013) which offers a weaker prediction than k-ω turbulence model.

$$\frac{\partial(\rho k)}{\partial t}+\frac{\partial}{\partial x_j}\left(\rho U_j k\right)=\frac{\partial}{\partial x_j}\left[\frac{\left(\mu+\frac{\mu_t}{\sigma_k}\right)\partial k}{\partial x_j}\right]+P_k-\beta'^{*}\rho k\omega \quad (1)$$

$$\frac{\partial(\rho\omega)}{\partial t}+\frac{\partial}{\partial x_j}\left(\rho U_j \omega\right)=\frac{\partial}{\partial x_j}\left[\frac{\left(\mu+\frac{\mu_t}{\sigma_k}\right)\partial \omega}{\partial x_j}\right]+P_\omega-\beta\rho\omega^2 \quad (2)$$

$$\mu_t=\frac{\rho k}{\omega} \quad (3)$$

In the above equations, ρ is the density, μ is the dynamic viscosity, k is the kinetic turbulence energy, ω is the frequency, U is the velocity vector, p_k is turbulence production rate, σ_ω=2, β'=0.09, α=5/9, β=0.075 and σ_k=2. The solved equations include the following equations:

Conservation of mass:

$$\frac{\partial\rho}{\partial t}+\vec{\nabla}.\left(\rho\vec{v}\right)=0 \quad (4)$$

Conservation of momentum:

$$\rho\frac{\partial\vec{v}}{\partial t}=\rho.(\vec{v}.\nabla)\vec{v}=-\nabla p+\nabla.\tau+\rho\vec{g} \quad (5)$$

Conservation of energy:

$$\frac{\partial(\rho h_{tot})}{\partial t}-\frac{\partial p}{\partial t}+\nabla.\left(\rho\vec{v}h_{tot}\right)=\nabla.\left(\lambda\nabla T\right)+\nabla.\left(\vec{v}.\tau\right) \quad (6)$$

$$h_{tot}=h+\frac{1}{2}U^2 \quad (7)$$

in which htot is the total enthalpy which is a function of pressure and temperature and the term $\nabla.(\vec{v}.\ \tau)$ shows the work done by viscosity-related stresses. This term causes internal heat due to the fluid viscosity which can be neglected in most flows.

5. MESH INDEPENDENCY

To ascertain the independency of the grid, four different types of grid has been generated on the geometry and the results were compared according to pressure value and efficiency. Finally, the value of 2465334 was used as the optimum value of the grid.

Table 2 Mesh independency

Mesh element	Efficiency	Total pressure ratio
1865257	0.7801	1.39
2022125	0.7925	1.424
2465334	0.8012	1.465
2627856	0.803	1.463

$$Pr=\frac{P_{total\ out}}{P_{total\ in}} \quad (8)$$

$$\eta_{tot}=\frac{\left(\left(\frac{P_{out}}{P_{in}}\right)^{\left(\frac{\gamma-1}{\gamma}\right)}-1\right)}{\frac{T_{out}}{T_{in}}} \quad (9)$$

Equations (8) and (9) are, respectively, related to the total pressure and isentropic efficiency of the axial compressor stage.

6. GEOMETRY MODELING

To investigate the geometry of rotor blade in the blade tip, and tip clearance on the performance of compressor stage, two geometries were proposed so that it could be compared with the rotor standard model having no change in the height of blade tip clearance. Figure 4 shows the geometries related to the compressor rotor. A change of geometry in the rotor blade tip causes various types of blade tip clearances.

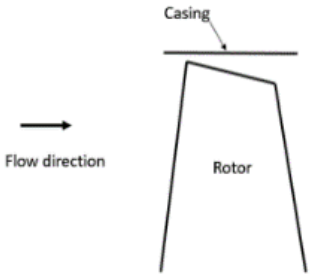

a) Model #1

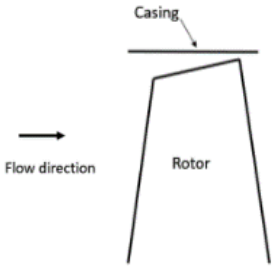

a) Model #2

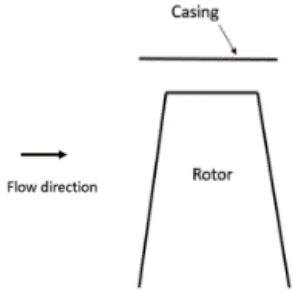

a) Model #3

Fig. 4. A view of the geometry of rotor with different tip clearance.

The geometries related to the blade tip have been created with respect to the lowest allowable value related to the blade tip distance to the casing wall, in a manner that the lowest allowable value of blade tip clearance was set as 0.06 mm and the average distance from the casing to the blade tip was set equal to 0.5 mm, as depicted in Fig. 5.

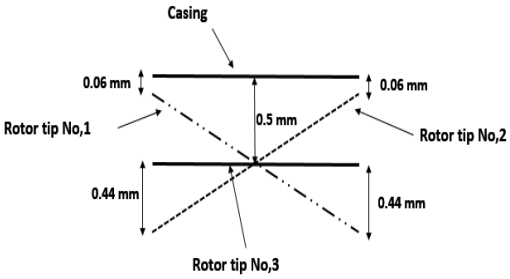

Fig. 5. Distance from the rotor tip to casing in various tip clearance.

7. NUMERICAL ANALYSIS

After creating 3-D geometries of the considered rotors, a mesh was applied on the geometry and then fed into the software for numerical analysis. It should be noted that to better simulate the geometry related to the compressor stage, the blades geometry was created using the fillet modeling of blade root. Figure 6, shows a view of the fillet in the stator blade root.

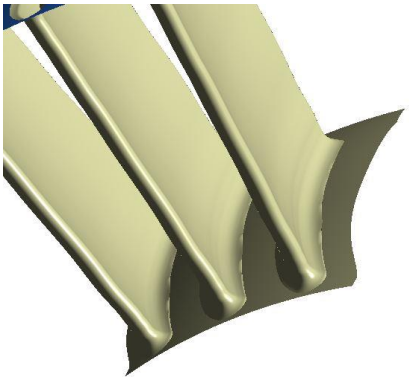

Fig. 6. A view of the fillet of stator.

The boundary conditions at the inlet of compressor are stagnation pressure and temperature which are, respectively, equal to 0.884 bar and 284 K. The turbulence intensity at the compressor inlet was considered as 1% because of using bellmouth at the inlet of compressor. Moreover, at the compressor outlet, by the application of variable static pressure, compressor performance charts were gradually obtained. The solutions were solved as transient with 0.00001 time step and 5 loop to give more precise result.

8. VALIDATION

The results obtained from the numerical simulation were compared against the experimental values as verification, shown in Figs. 7 and 8. As previously mentioned, the numerical analysis results were verified against the experimental values at a rotational speed of 28015 revolutions per minute. The maximum computational error was 9%. Because of high rotational speed and complexity of inside flow, discrepancy between experimental and numerical data was a little high. The trend of pressure ratio curve obtained from numerical analysis approximately corresponds to that of experimental values.

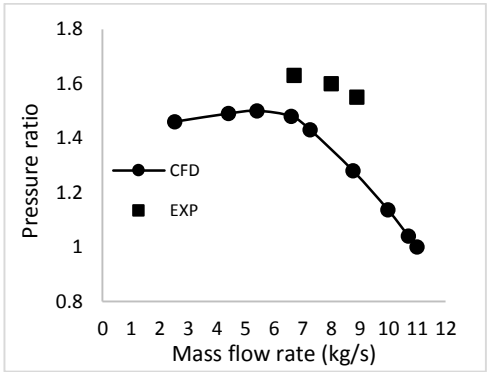

Fig. 7. Results of total pressure in standard model (model #3) for numerical solution compared with the experimental results.

Figure 8, shows the results of isentropic efficiency for numerical solution compared with the experimental results. As can be seen, the numerical values have a good agreement with the experimental data.

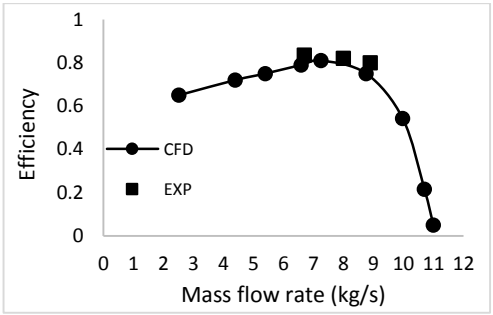

Fig. 8. Results of isentropic efficiency for numerical solution compared with the experimental results.

9. ANALYSIS OF THE RESULTS

The results of numerical analysis in the three considered models show that the tip clearance of the first model (model #1) has the biggest effect on the compressor performance loss. Figure 9 is related to the comparison of pressure ratio in the three studied rotor models. It can be noticed that the results belonging to the first model, present the biggest loss in the stall margin where with decreasing mass flow rate, the pressure ratio would decrease. The third rotor (model #3) has the best performance in the region related to the stall margin. The second rotor (model #2) shows itself somewhere between the other two models.

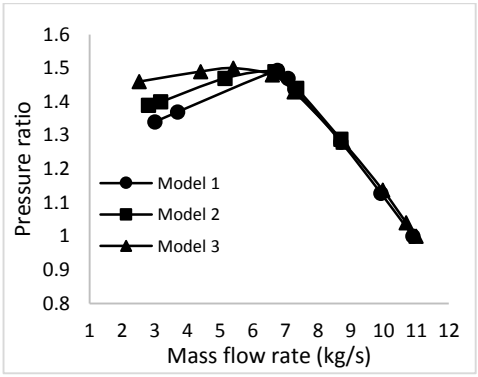

Fig. 9. Comparison of pressure ratio in the three studied rotor models.

It is also evident from the isentropic efficiency graph, Fig. 10, that the biggest loss exists in the second model and the efficiency has decreased than the third standard model (standard model #3).

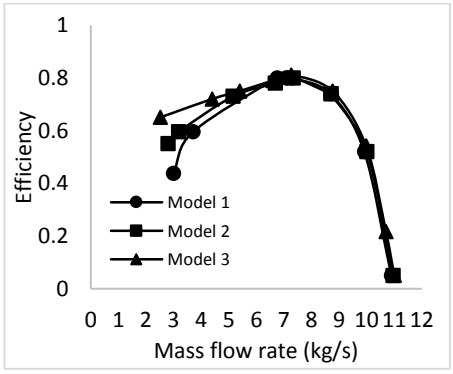

Fig. 10. Isentropic efficiency graph in the three studied rotor models.

The change of blade tip clearance has shown to have an effect on the outlet flow angle. As is shown in Fig. 11, the biggest deviation of angle is related to the model #1. This deviation of angle, causes flow separation in the next compressor stages and reduction of compressor efficiency.

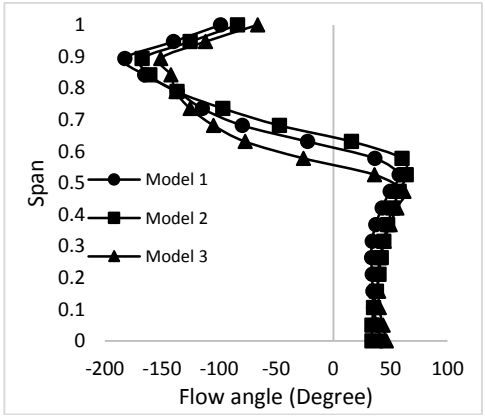

Fig. 11. Contour of outlet flow angle from the rotor stage in stall configuration.

The contours of outlet flow angle from the rotor stage in the maximum efficiency state, Fig. 12, also depict the maximum angle change for model #1 and the highest amount of this change in angle is located in the region close to the blade tip. This black region observed in Fig. 12(a), is a sign of tip clearance model #1 intense effect on the rotor outlet flow. Also the Model#2 has two critical regions at the tip. The best condition about the outlet flow angle is specified to Model #3 with minimum flow deviation.

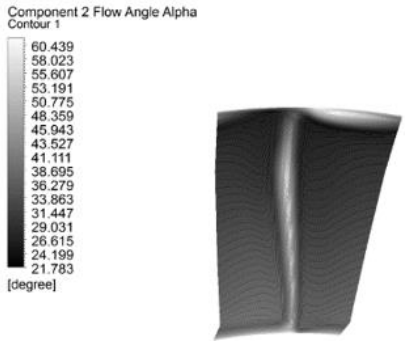

a) Model #1

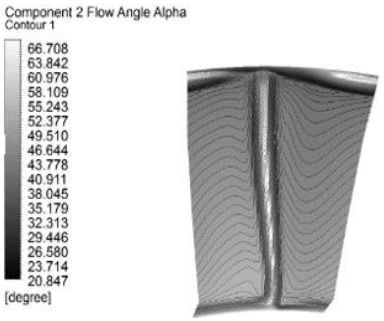

b) Model #2

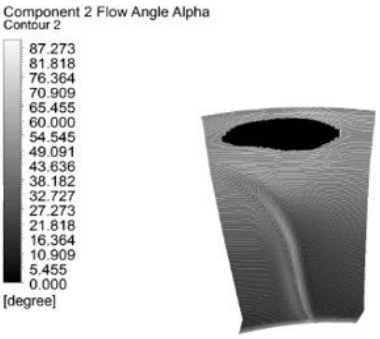

c) Model #3

Fig. 12. Contour of outlet flow angle from the rotor stage in various models in the maximum efficiency.

The contours related to velocity in the meridional view for the maximum efficiency state, exhibit the highest velocity reduction which is related to the black spots in Fig. 13. The maximum decrease in velocity belongs to the model #1. The increase of low-velocity regions triggers the stall cells and even surge phenomenon in critical conditions. Blade tip clearance clearly exhibits its effect on the compressor performance in critical conditions. In this situation, the impact of tip clearance geometry change on the performance of the compressor is obvious.

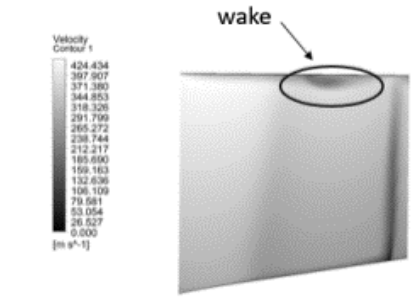

a) Model #1

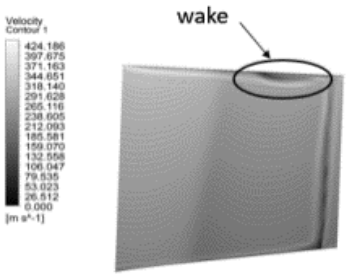

b) Model #2

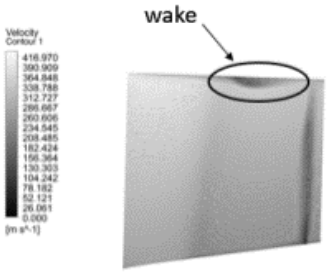

c) Model #3

Fig. 13. Contours related to axial velocity in the meridional view for the maximum efficiency state.

Since the pressure gradient increases as the flow moves toward downstream, the total pressure significantly rises while the flow moves from the rotor inlet to its outlet. This pressure rise can be attributed to the kinetic energy absorption from the rotor's shaft rotation. As a result, for the tip clearance regions where it is not able to transfer kinetic energy from the blade tip to the flow, the flow leaks from the blade tip, which is known as tip leakage flow. The leaked flow from the blade tip, experiences a separation and reduces the compressor performance as it lacks enough kinetic energy against the adverse pressure gradient.

In the first model rotor, since the tip clearance increases as it approaches the trailing edge, and also because of adverse pressure gradient rise by moving toward the rotor blade trailing edge, more flow leaks from the blade tip in rotor blade tip trailing edge region, hence resulting in considerable stall cell in the rotor domain which further reduces the efficiency and compressor performance.

By inspecting model #2, as the maximum tip clearance exists in the rotor leading edge, less flow leaks from the blade tip edge and this can be attributed to less pressure gradient in blade leading edge compared in its trailing edge, so that the stall cell is smaller in this case than model #1.

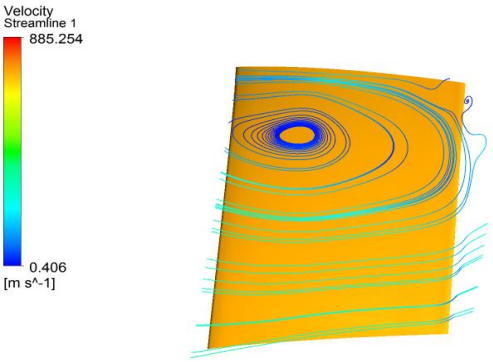

Fig. 14. Stall cell in suction surface of rotor #1.

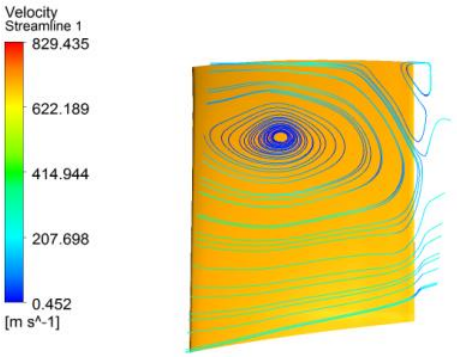

Fig. 15. Stall cell in suction surface of rotor #2.

In the rotor belonging to model #3, the separation is not as strong as other states and it has little effect in stall compared with the rotors of model #1 and #2, Fig. 16. Therefore, the smallest stall cell in critical condition is associated to model #3.

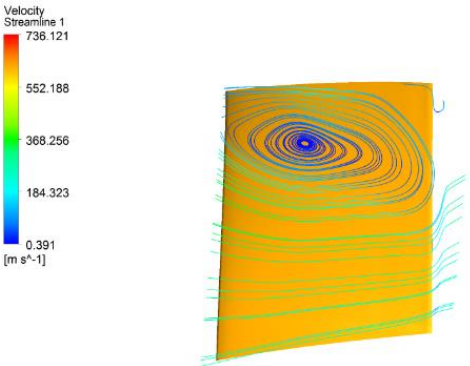

Fig. 16. Stall cell in suction surface of rotor #2.

10. CONCLUSION

In this article, the original blade with constant tip clearance was verified by experimental data. After verifying the numerical model, two geometries were created by modifying the tip clearance geometry, and then compared with the standard model. The results have shown that the maximum value of tip clearance existing in the trailing edge (model #1) corresponds

to the maximum compressor performance and causes more flow deviation from the rotor. More suitable conditions exist for model #2, but it still ranks behind the standard model in terms of performance. The results also showed that modifying the blade tip geometry is not an appropriate method to increase the compressor efficiency and the existence of variable blade tip clearance height, is not a suitable idea to improve the compressor performance.

REFERENCES

Bae, J.W., K.S. Breuer and C.S. Tan (2003). Active control of tip clearance flow in axial compressors. *ASME Turbo Expo, collocated with the 2003 International Joint Power Generation Conference 6*, 531-542.

Bianchi, S., A. Corsini, F. Rispoli and A.G. Sheard (2008). Experimental aeroacoustic studies on improved tip geometries for passive noise signature control in low-speed axial fan. *ASME Turbo Expo: power for land, sea and air* 6, 863-875.

Corsini, A., B. Perugini, F. Rispoli, A.G. Sheard and I.R. Kinghorn (2006). Investigation on improved blade tip concept for axial flow fan. *ASME Turbo Expo: power for land, sea and air* 6, 313-325.

Corsini, A., F. Rispoli and A.G. Sheard (2008). Shaping of tip end-plate to control leakage vortex swirl in axial flow, *ASME Turbo Expo: power for land, sea and air* 6, 571-580.

Domercq, O. and J. F. Escuret (2007). Tip clearance effect on high-pressure compressor stage matching. *Proceedings of the Institution of Mechanical Engineers, Part A: Journal of Power and Energy* 221(6), 759–767.

Foley, A.C. and P.C. Ivey (1996). Measurement of tip-clearance flow in a multistage, axial flow compressor. *Journal of Turbomachinery* 118(2), 211–217.

Han, S. and J. Zhong (2011). The influences of pressure-side winglet on aerodynamic performance of compressor cascade at different incidences. *International Conference on Consumer Electronics, Communications and Networks (CECNet)*, XianNing, China.

Howard, M. A., P. C. Ivey, J. P. Barton and K. F. Young (1994). Endwall effects at two tip clearances in a multistage axial flow compressor with controlled diffusion blading. *Journal of Turbomachinery* 116(4), 635–645.

Kim, J. H., K. J. Choi and K. Y. Kim (2013). Aerodynamic analysis and optimization of a transonic axial compressor with casing grooves to improve operating stability, *Aerospace Science and Technology* 29(1), 81-91.

Kroger, G., C. Voß, E. Nicke and C. Cornelius (2011). Theory and application of axisymmetric endwall contouring for compressors. *ASME Turbo Expo: Turbine Technical Conference and Exposition* 7, 125-137.

Sitaram, N. and G. Ch. V. Sivakumar (2011). Effect of partial shrouds on the performance and flow field of a low-aspect-ratio axial-flow fan rotor. *International Journal of Rotating Machinery*.

Smith, N. R. and N. L. Key (2015). Flow visualization for investigating stator losses in a multistage axial compressor. *Experiments in Fluids* 56, 1–17.

Zhong J., H. Shaobing, L. Huawei, K. Xiaoxu (2013). Effect of tip geometry and tip clearance on aerodynamic performance of a linear compressor cascade. *Chinese Journal of Aeronautics* 26(3), 583–593.

Zhong, J., S. Han and P. Sun (2011). The influence of suction-side winglet on tip leakage flow in compressor cascade. *ASME Turbo Expo: Turbine Technical Conference and Exposition* 7, 263-273.